# Discrete-Time AUV Tracking Controller Design Based on Disturbance Rejection and Dynamic Trajectory Planning

Remon Al Azrak[†,*], Kai Treichel[†] and Johann Reger[†]

***Abstract*—In this work, we discuss a flexible on-line trajectory planning algorithm for autonomous underwater vehicles. For dynamically allocated way-points and surge velocities, an on-line algorithm computes polynomials that smoothly link the paths between these way-points, based on the kinematics of the vehicle. We devise a tracking controller that compensates for the nonlinearities of the rigid body dynamics in order to render it linear in closed-loop. For the attenuation of large disturbances an extended state observer is employed that helps improve the tracking performance. Simulation studies on real-world vehicle data underscore the usuablity of the advocated approach.**

## I. INTRODUCTION

The wide range of applications of autonomous underwater vehicles (AUV) in hard and risky environments, such as the exploration of oil and other underwater resources, inspection and studying of the water quality and fish feeding, has made AUV a very attractive field of study in robotics and control research in the past two decades [1], [2], [3]. It is the nature of these applications, that the planning, automation and control of the corresponding maneuvers often turn out demanding tasks. Parts of them, usually, are relegated to maneuver processors. They supply information about the way-points to the path planner which generates, in turn, the suitable trajectories for the motion. The information may be provided remotely or can be stored into the system such that the trajectories generation can be made off-line [4].

In this paper, we discuss an algorithm for the smooth on-line path and trajectory planning of AUV manuevers. To this end, the algorithm is based on piecewise polynomials of degree 5. For the trajectory generation the algorithm initially requires the information of four way-points, only, and then just the information about each new way-point. The procedure yields some flexibility during the path planning when sudden changes in the environment occur. The trajectories planning is investigated for three kinds of underwater motions, namely: vertical, 2D and 3D. The second part of this contribution is the design of a controller which guarantees acceptable tracking performance for the generated trajectories. The design idea is first to compensate all the nonlinear terms of the vehicle dynamics and then to design a suitable discrete PD- or PID-controller for forcing the error dynamics to asymptotically converge to zero. Whenever the system is not perturbed, it is well-known that a conventional PD-controller may do the task. For the more realistic perturbed case, we advocate the use of a GESO approach (Generalized Extended State Observer) for the online estimation and attenuation of the disturbance-induced adverse effects in order to improve the performance and stability of the closed-loop system.

The contribution is structured as follows: After briefly recalling the AUV dynamics in Section II, the real-time path and trajectory planning algorithm is exposed in Section III. Section IV presents the nominal tracking controller design which is enhanced by a GESO disturbance rejection scheme in Section V. Simulation results on real-world AUV data in Section VI illustrate the usability of the afore-developed approach. Section VII closes the paper with conlusions and perspectives for further work.

## II. UNDERWATER VEHICLE DYNAMICS

The equations of motion of an AUV, typically, is described by a rigid body movement in viscous media (see [5], [6]), i.e. a set of non-linear differential equations of the form

$$\Sigma : \begin{cases} M\dot{\nu} + C(\nu)\nu + D(\nu)\nu + g(\eta) = \tau \\ \dot{\eta} = J(\eta)\nu \end{cases} \tag{1}$$

where $M$ is the inertia matrix (constant for low velocities), $C(\nu)$ the matrix of Coriolis and centripetal terms (including added mass), $D(\nu)$ the viscous damping matrix, $g(\eta)$ the vector of gravitational (also buoyancy) forces/moments and $\tau$ the vector of control inputs acting on the vehicle in the body-fixed frame. The vector $\eta = [x, y, z, \phi, \theta, \psi]^{\mathrm{T}}$ denotes the position and orientation in earth-fixed frame, whereas the vector $\nu = [u, v, w, p, q, r]^{\mathrm{T}}$ denotes the linear and angular velocity in body-fixed frame. As usual, $J(\eta)$ is the transformation matrix between the body-fixed frame and earth-fixed frame. Fig. 1 depicts the relation of the body-fixed frame $O - X_0Y_0Z_0$, attached to the vehicle, to the earth-fixed frame $XYZ$. The origin of the body-fixed frame is chosen to coincide with the center of gravity of the moving vehicle. The directions are as follows [6]:

$X_0$: longitudinal axis (directed from aft to fore)
$Y_0$: transverse axis (directed to starboard)
$Z_0$: normal axis (directed from top to bottom)

[†]*Control Engineering Group, Ilmenau University of Technology, Helmholzplatz 5, D-98693 Ilmenau, Germany.* E-mails: remon.al-azrak@tu-ilmenau.de, kai.treichel@tu-ilmenau.de, reger@ieee.org.

[*]Work of Remon Al Azrak was partially supported by the European Regional Development Fund (ERDF) of the European Union via the Thuringian Coordination Office TNA #TNA VIII-1/2011

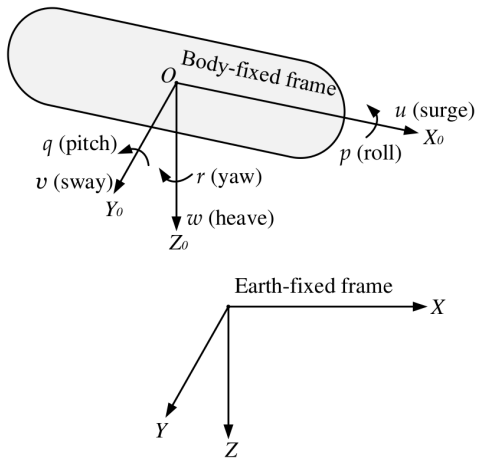


Fig. 1. Body-fixed and earth-fixed reference frames

Thus, $(u, v, w)$ are the translation velocities in body-fixed frame coordinates and $(p, q, r)$ the respective angular velocities related to $X_0, Y_0, Z_0$. For zero velocities in sway and heave ($v \equiv 0$ and $w \equiv 0$) the kinematics of the moving vehicle, that is $\dot{\eta} = J(\eta)\nu$ from (1), may be expressed in the following six differential equations [7]:

$$\dot{x} = u\cos(\theta)\cos(\psi) \quad (2)$$

$$\dot{y} = u\cos(\theta)\sin(\psi) \quad (3)$$

$$\dot{z} = -u\sin(\theta) \quad (4)$$

$$\dot{\phi} = p + q\sin(\phi)\tan(\theta) + r\cos(\phi)\tan(\theta) \quad (5)$$

$$\dot{\theta} = q\cos(\phi) - r\sin(\phi) \quad (6)$$

$$\dot{\psi} = q\frac{\sin(\phi)}{\cos(\theta)} + r\frac{\cos(\phi)}{\cos(\theta)} \quad (7)$$

## III. PATH AND TRAJECTORY PLANNING

In this section, we consider vertical maneuvers, 2D- and 3D maneuvers of the AUV.

### A. Vertical Maneuver

We assume that the initial and final positions as well as the initial and final orientations (zero roll) are given for two way-points $(\mathbf{x}_0, \mathbf{y}_0, \mathbf{z}_0)$ and $(\mathbf{x}_0, \mathbf{y}_0, \mathbf{z}_\mathrm{f})$. To the end of a smooth transition, a polynomial of degree 5 is adopted to satisfy six boundary conditions (in position, velocity, and acceleration). Therefore, a stationary rest to rest transition from $z(t_0) = \mathbf{z}_0$ and $z(t_\mathrm{f}) = \mathbf{z}_\mathrm{f}$ with zero boundary values for velocity and acceleration determines the six coefficients of the polynomial

$$z(t) = \alpha_5(t-t_0)^5 + \alpha_4(t-t_0)^4 + \alpha_3(t-t_0)^3 + \alpha_2(t-t_0)^2 + \alpha_1(t-t_0) + \alpha_0\,. \quad (8)$$

For unknown final time $t_\mathrm{f}$ the coefficients may be obtained by introducing a maximum value of the heave velocity for the vertical motion $w_\mathrm{max}$, reached at time $(t_\mathrm{f} - t_0)/2$. In this case, see [8], we have $t_f = \frac{15(\mathbf{z}_\mathrm{f}-\mathbf{z}_0)}{8w_\mathrm{max}}$ and with $T_z = t_\mathrm{f} - t_0$, $h_z = \mathbf{z}_f - \mathbf{z}_0$ the coefficients are given as:

$$\alpha_5 = \frac{12h_z}{2T_z^5},\ \alpha_4 = \frac{-30h_z}{2T_z^4},\ \alpha_3 = \frac{20h_z}{2T_z^3},\ \alpha_2 = \alpha_1 = 0,\ \alpha_0 = \mathbf{z}_0\,. \quad (9)$$

Subject to the same assumptions, similarly, the trajectories for the angles $\theta(t)$ and $\psi(t)$ may be determined. For example, the transition between the yaw angles $\boldsymbol{\psi}_0$ and $\boldsymbol{\psi}_\mathrm{f}$ may be planned with polynomial

$$\psi(t) = \beta_5(t-t_0)^5 + \beta_4(t-t_0)^4 + \beta_3(t-t_0)^3 + \beta_2(t-t_0)^2 + \beta_1(t-t_0) + \beta_0 \quad (10)$$

where the coefficients are

$$\beta_5 = \frac{12h_\psi}{2T_z^5},\ \beta_4 = \frac{-30h_\psi}{2T_z^4},\ \beta_3 = \frac{20h_\psi}{2T_z^3},\ \beta_2 = \beta_1 = 0,\ \beta_0 = \boldsymbol{\psi}_0 \quad (11)$$

with $h_\psi = \boldsymbol{\psi}_\mathrm{f} - \boldsymbol{\psi}_0$ and $t_\mathrm{f}$, when unknown, determined from $w_\mathrm{max}$ as above.

This way we may design the desired trajectories $z(t)$, $\psi(t)$, and $\phi(t)$ just involving the initial and final values of position and orientation, and if need be, the maximum value of $w$. At the end of this maneuver the AUV is located at the stationary point $(\mathbf{x}_0, \mathbf{y}_0, \mathbf{z}_\mathrm{f})$ with orientation $(0, \boldsymbol{\theta}_\mathrm{f}, \boldsymbol{\psi}_\mathrm{f})$, as desired.

### B. 2D- and 3D-maneuver

Based on the kinematics (2) to (7) and under the assumption of zero roll, $\phi \equiv 0$, trajectories may be designed for a path, which passes through a certain set of Cartesian way-points $(\mathbf{x}_k, \mathbf{y}_k, \mathbf{z}_k)$, with $k = 0, 1, \ldots, N-1$, where $N$ is the number of way-points. To this end, by introducing a path variable $\Theta$ we get the parameterized path $(x_\mathrm{d}(\Theta), y_\mathrm{d}(\Theta), z_\mathrm{d}(\Theta))$ using a polynomial of degree 5 interpolation of the pre-defined way-points [8], and subsequently may determine $\Theta$ as a function of time in order to match the desired surge velocity profile in the path planning procedure [4].

A challenge here is how to generate an appropriate path when new way-points are added on-line to the predefined way-points, that is, during the mission. Four way-points are needed to generate a twice continuously differentiable function of $\Theta$ that satisfies the boundary conditions for the velocity and acceleration in the way-points. Therefore, polynomials of fifth degree are generated iteratively, considering only four way-points in each iteration. In each iteration, just the first polynomial (between the first and the second point) is regarded, and the two polynomials (between second way-point and third way-point) as well as the polynomial (between third way-point and fourth way-point) are neglected as long as the fourth way-point is not the last one in the mission. Iteratively, we get a polynomial for each new added way-point to the path. When the last point of the path is reached then the three polynomials interpolated between the four considered way points are taken into account. In other words, for all iterations just one polynomial is regarded, but for the last iteration three polynomials need to be regarded. Fig. 2 illustrates the algorithm for the generation of the polynomial $x_\mathrm{d}(\Theta)$ referring

to $N = 6$ way-points: In the first iteration $j = 1$ just $a_0^1$ is considered, for $j = 2$ just $a_1^2$ is considered, but in the last iteration $j = 3$ are $a_2^3, a_3^3$ and $a_4^3$ considered. Therefore, the parameter vectors $a_0^1, a_1^2, a_2^3, a_3^3$ and $a_4^3$ represent the function between way-point $\mathbf{x}_0$ and way-point $\mathbf{x}_5$. Since the vectors $a_0^1$, $a_1^1$ and $a_2^1$ are provided from the first iteration it is possible to calculate the velocities and accelerations in the via points $\mathbf{x}_1$ and $\mathbf{x}_2$. The velocity and acceleration in the first via point (in the first iteration) is valid as a start velocity and start acceleration for the second one, and the velocity and acceleration in the first via point (in the second iteration) is valid as a start velocity and start acceleration for the third one, and so forth. That means, that the boundary conditions for velocity and acceleration are guaranteed in each way-point, and subsequently, we get a twice continuously differentiable function between the way-point $\mathbf{x}_0$ and the way-point $\mathbf{x}_5$. Thus, we can extend this algorithm for $N$ way-points to get the desired polynomial $x_\mathrm{d}(\Theta)$. The same algorithm is applied

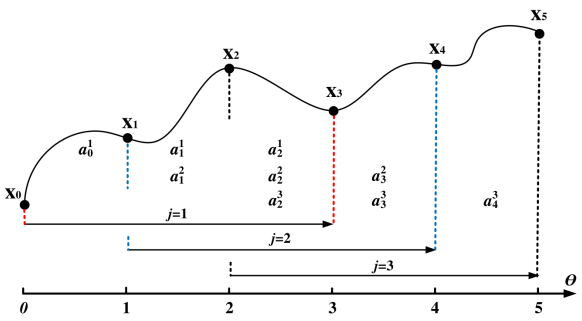


Fig. 2. On-line path planning

to obtain parameter vectors for the polynomials $y_\mathrm{d}(\Theta)$ and $z_\mathrm{d}(\Theta)$. The afore-presented algorithm can be generalized to determine a path in 3D-space, that means, we need three polynomials of degree five:

$$x_{i,\mathrm{d}}^j(\Theta) = a_{i,5}^j\Theta^5 + a_{i,4}^j\Theta^4 + a_{i,3}^j\Theta^3 + a_{i,2}^j\Theta^2 + a_{i,1}^j\Theta + a_{i,0}^j \tag{12}$$

$$y_{i,\mathrm{d}}^j(\Theta) = b_{i,5}^j\Theta^5 + b_{i,4}^j\Theta^4 + b_{i,3}^j\Theta^3 + b_{i,2}^j\Theta^2 + b_{i,1}^j\Theta + b_{i,0}^j \tag{13}$$

$$z_{i,\mathrm{d}}^j(\Theta) = c_{i,5}^j\Theta^5 + c_{i,4}^j\Theta^4 + c_{i,3}^j\Theta^3 + c_{i,2}^j\Theta^2 + c_{i,1}^j\Theta + c_{i,0}^j \tag{14}$$

with the parameter vectors in the $j$th iteration

$$\begin{aligned} a_i^j &= [a_{i,5}^j \;\; a_{i,4}^j \;\; a_{i,3}^j \;\; a_{i,2}^j \;\; a_{i,1}^j, \;\; a_{i,0}^j] \\ b_i^j &= [b_{i,5}^j \;\; b_{i,4}^j \;\; b_{i,3}^j \;\; b_{i,2}^j \;\; b_{i,1}^j, \;\; b_{i,0}^j] \\ c_i^j &= [c_{i,5}^j \;\; c_{i,4}^j \;\; c_{i,3}^j \;\; c_{i,2}^j \;\; c_{i,1}^j, \;\; c_{i,0}^j] \end{aligned}$$

where $i$ is the index of the first way-point form the four considered way-point in the iteration $j$ with $j = 1 \ldots N-3$, where $N$ the number of the way-points. Note that the index $i$ starts at the value $i = j - 1$. For example, for the iteration index $j = 2$ the indices of the regarded four way-points are $1, 2, 3$ and $4$. For each iteration $j$ the four way-points $\mathbf{x}_i, \mathbf{x}_{i+1}, \mathbf{x}_{i+2}, \mathbf{x}_{i+3}$ are considered to obtain the coefficients for the three polynomials between those points regarding to the boundary conditions in each way-point as well as in start and end way-points. Obviously, the desired trajectories $x_\mathrm{d}(\Theta)$, $y_\mathrm{d}(\Theta)$ and $z_\mathrm{d}(\Theta)$ then, in a piecewise manner, consist of the polynomials $x_{i,\mathrm{d}}^j(\Theta)$, $y_{i,\mathrm{d}}^j(\Theta)$ and $z_{i,\mathrm{d}}^j(\Theta)$.

This procedure leads to introduce the invertible parameter matrix $P \in \mathbb{R}^{18\times 18}$:

$$P(\Theta_i^j, \ldots \Theta_{i+3}^j) = \left(\begin{array}{ccc} \mathbf{a}(\Theta_i^j) & O & O \\ \mathbf{v}(\Theta_i^j) & O & O \\ \mathbf{p}(\Theta_i^j) & O & O \\ \hline \mathbf{p}(\Theta_{i+1}^j) & O & O \\ O & \mathbf{p}(\Theta_{i+1}^j) & O \\ -\mathbf{v}(\Theta_{i+1}^j) & \mathbf{v}(\Theta_{i+1}^j) & O \\ -\mathbf{a}(\Theta_{i+1}^j) & \mathbf{a}(\Theta_{i+1}^j) & O \\ -\mathbf{r}(\Theta_{i+1}^j) & \mathbf{r}(\Theta_{i+1}^j) & O \\ -\mathbf{s}(\Theta_{i+1}^j) & \mathbf{s}(\Theta_{i+1}^j) & O \\ \hline O & \mathbf{p}(\Theta_{i+2}^j) & O \\ O & O & \mathbf{p}(\Theta_{i+2}^j) \\ O & -\mathbf{v}(\Theta_{i+2}^j) & \mathbf{v}(\Theta_{i+2}^j) \\ O & -\mathbf{a}(\Theta_{i+2}^j) & \mathbf{a}(\Theta_{i+2}^j) \\ O & -\mathbf{r}(\Theta_{i+2}^j) & \mathbf{r}(\Theta_{i+2}^j) \\ O & -\mathbf{s}(\Theta_{i+2}^j) & \mathbf{s}(\Theta_{i+2}^j) \\ \hline O & O & \mathbf{a}(\Theta_{i+3}^j) \\ O & O & \mathbf{v}(\Theta_{i+3}^j) \\ O & O & \mathbf{p}(\Theta_{i+3}^j) \end{array}\right)$$

with

$$\mathbf{p}(\Theta_i^j) = \begin{pmatrix} (\Theta_i^j)^5 & (\Theta_i^j)^4 & (\Theta_i^j)^3 & (\Theta_i^j)^2 & \Theta_i^j & 1 \end{pmatrix}, \tag{15}$$

$$\mathbf{v}(\Theta_i^j) = \begin{pmatrix} 5(\Theta_i^j)^4 & 4(\Theta_i^j)^3 & 3(\Theta_i^j)^2 & 2\Theta_i^j & \Theta_i & 0 \end{pmatrix}, \tag{16}$$

$$\mathbf{a}(\Theta_i^j) = \begin{pmatrix} 20(\Theta_i^j)^3 & 12(\Theta_i^j)^2 & 6\Theta_i^j & 2 & 0 & 0 \end{pmatrix} \tag{17}$$

$$\mathbf{r}(\Theta_i^j) = \begin{pmatrix} 60(\Theta_i^j)^2 & 24(\Theta_i^j) & 6 & 0 & 0 & 0 \end{pmatrix} \tag{18}$$

$$\mathbf{s}(\Theta_i^j) = \begin{pmatrix} 120(\Theta_i^j) & 24 & 0 & 0 & 0 & 0 \end{pmatrix} \tag{19}$$

$$O = \begin{pmatrix} 0 & 0 & 0 & 0 & 0 & 0 \end{pmatrix}. \tag{20}$$

for determining the vector of polynomial coefficients $X_\mathrm{coff}^j$ as a solution of a linear system of equations in terms of the way-point vector in the $j$th iteration, $X_{way}^j$. Hence,

$$X_\mathrm{coff}^j = P^{-1} X_\mathrm{way}^j \tag{21}$$

with

$$\begin{aligned} X_{way}^j = (&\mathbf{a}_i, \mathbf{v}_i, \mathbf{x}_i, \mathbf{x}_{i+1}, \mathbf{x}_{i+1}, 0, 0, 0, 0, \\ &\mathbf{x}_{i+2}, \mathbf{x}_{i+2}, 0, 0, 0, 0, 0, 0, \mathbf{x}_{i+3})^\mathrm{T}. \end{aligned}$$

Note first, that the start velocity $\mathbf{v}_i$ as well as the start acceleration $\mathbf{a}_i$ can be calculated form the previous iteration, and second, that the end velocity and end acceleration for

each iteration is zero. With this consideration we can define a frame with specific properties to be shifted over the whole range of the way-points, iteratively, where initial values of velocity and acceleration at the start of the mission can be set by the user, and the final velocity and acceleration are set to zero, i.e. "end of the mission". Thus, for a mission consisting of four way-points in the $j$-th iteration, we obtain a vector of $18$ polynomial coefficients and the intermediate path will be described through three resulting polynomials. Once a new way-point is available, only the first polynomial is regarded and the two others are neglected such that the algorithm may be iterated again for four way-points. The first three of them are the last three points of the previous iteration and the fourth one is the new added way-point. The iteration starts from the $(i+1)$-th way-point and ends in the $(i+5)$-th way-point. It means that for any new way-point added on-line to the path a suitable intermediate path will be generated.

*Remark 1:* It is useful to notice that, in practice, numerical problems may arise when computing the inverse of the parameter matrix $P$. For reducing these problems, the coefficients of the polynomials may alternatively be determined using the so-called Bézier-Bernstein polynomials, see [8].

For a 2D-maneuver, polynomials (12) and (13) are considered to generate the desired path that passes through the given way-points in the Cartesian plane. Such a path is transformed to a time dependent trajectory by imposing the desired surge velocity profile $u_{\mathrm{d}}(t)$ (assuming roll and pitch equal to zero). It can be shown that $\Theta$ may be obtained as the solution of the scalar differential equation:

$$\dot{\Theta} = \frac{u_{\mathrm{d}}(t)}{\cos\psi_{\mathrm{d}}(\Theta)x'_{\mathrm{d}}(\Theta) + \sin\psi_{\mathrm{d}}(\Theta)y'_{\mathrm{d}}(\Theta)} \tag{22}$$

with $\Theta(0) = 0$, $(.)' = \frac{\partial}{\partial\Theta}(.)$ and $\psi_{\mathrm{d}}(\Theta) = \arctan\frac{y'_{\mathrm{d}}(\Theta)}{x'_{\mathrm{d}}(\Theta)}$. Finally, with the solution $\Theta = \Theta(t)$ we obtain a coordinate description in terms of time, hence trajectories, $x_{\mathrm{d}} = x_{\mathrm{d}}(t)$, $y_{\mathrm{d}} = y_{\mathrm{d}}(t)$ and $\psi_{\mathrm{d}} = \psi_{\mathrm{d}}(t)$.

For a 3D-maneuver, polynomials (12), (13), (14) and the kinematics (2) – (7) are required (supposing roll is zero). By means of the desired profile of the longitudinal velocity $u_{\mathrm{d}}(t)$, the time-dependent path variable $\Theta = \Theta(t)$ is obtained as the solution of the scaler differential equation [7]

$$\dot{\Theta} = \frac{u_{\mathrm{d}}(t)}{\sqrt{x'^2_{\mathrm{d}} + y'^2_{\mathrm{d}} + z'^2_{\mathrm{d}})}} \tag{23}$$

with $\Theta(0) = 0$. In view of

$$\theta_{\mathrm{d}}(\Theta) = \arctan\frac{-z'_{\mathrm{d}}(\Theta)}{\sqrt{((x'_{(}\Theta))^2 + (y'_{\mathrm{d}}(\Theta)))^2}}, \tag{24}$$

$$\psi_{\mathrm{d}}(\Theta) = \arctan\frac{y'_{\mathrm{d}}(\Theta)}{x'_{\mathrm{d}}(\Theta)} \tag{25}$$

we may eventually obtain the desired trajectories $x_{\mathrm{d}} = x_{\mathrm{d}}(t)$, $y_{\mathrm{d}} = y_{\mathrm{d}}(t)$, $z_{\mathrm{d}} = z_{\mathrm{d}}(t)$, $\theta_{\mathrm{d}} = \theta_{\mathrm{d}}(t)$, and $\psi_{\mathrm{d}} = \psi_{\mathrm{d}}(t)$.

## IV. Tracking Controller Design

These generated trajectories are imposed on the AUV dynamics invoking a discrete computed torque controller. To this end, based on the forward Euler discretization [4] a discrete 6 degrees of freedom nonlinear model is obtained from $\Sigma$. With a slight abuse of denotation from the continuous model, we may then express the discrete equations of motion as follows:

$$\eta(k+1) = \eta(k) + TJ(\eta(k))\nu(k) \tag{26}$$

$$\begin{aligned}\nu(k+1) = \nu(k) &- TM^{-1}(C(\nu(k)) + D(\nu(k)))\nu(k) \\ &- TM^{-1}g(\eta(k)) + TM^{-1}(\tau(k) + d(k))\end{aligned} \tag{27}$$

where $T$ denotes the sampling time and $d(k)$ an additional input (i.e. force) disturbance. After substituting (27) in the shifted version of (26) we obtain

$$\begin{aligned}\eta(k+2) = \eta(k+1) + TJ(\eta(k+1))\Big(&\nu(k) - TM^{-1}g(\eta(k)) \\ &- TM^{-1}(C(\nu(k)) + D(\nu(k)))\nu(k) + TM^{-1}(\tau(k) + d(k))\Big).\end{aligned} \tag{28}$$

Now, we devise the nominal controller (disturbance-free case, $d(k) \equiv 0$) such that with a new input $\gamma(k)$ the dynamics in closed-loop shows double integrating behaviour

$$\frac{1}{T^2}\big(\eta(k+2) - 2\eta(k+1) + \eta(k)\big) = \gamma(k)\,. \tag{29}$$

By comparison of (29) with (28) it follows that we need to choose the compensator as

$$\begin{aligned}\tau(k) = g(\eta(k)) &+ \Big(C(\nu(k)) + D(\nu(k)) - \frac{1}{T}M\Big)\nu(k) \\ &+ MJ^{-1}\big(\eta(k+1))\Big)\Big(\gamma(k) + \frac{1}{T}J(\eta(k))\nu(k)\Big)\end{aligned} \tag{30}$$

where the new input $\gamma(k)$ may be chosen as a nominal discrete PD-controller with feed-forward term, say $\gamma(k) = \bar{\gamma}(k)$, which for the tracking in the nominal case turns out to be sufficient. Hence with $K_{\mathrm{P}}, K_{\mathrm{D}} \in \mathbb{R}^{6\times 6}$ as gain matrices the nominal PD-controller reads

$$\begin{aligned}\bar{\gamma}(k) = \frac{1}{T^2}\big(\eta_{\mathrm{d}}(k+2) - 2\eta_{\mathrm{d}}(k+1) + \eta_{\mathrm{d}}(k)\big) - K_{\mathrm{P}}(\eta(k) - \eta_{\mathrm{d}}(k)) \\ - \frac{K_{\mathrm{D}}}{T}\big(\eta(k+1) - \eta(k) - \eta_{\mathrm{d}}(k+1) + \eta_{\mathrm{d}}(k)\big)\,.\end{aligned} \tag{31}$$

Note that in this equation as well as in (30) expression $\eta(k+1)$ may be expressed in variables at instant $k$ using equation (26).

In order to asses the values of the gains, we may substitute $\bar{\gamma}(k)$ in (29) which then yields the dynamics in terms of the error $e(k) = \eta(k) - \eta_{\mathrm{d}}(k)$, i.e.

$$e(k+2) + (TK_{\mathrm{D}} - 2I)e(k+1) + (I + T^2K_{\mathrm{P}} - TK_{\mathrm{D}})e(k) = 0 \tag{32}$$

with $I \in \mathbb{R}^{6\times 6}$ the identity matrix. Choosing diagonal gains for supressing the error coupling, equation (32) may be rewritten as the $i = 1, \ldots, 6$ equations

$$e_i(k+2) + (TK_{\mathrm{D},i} - 2)e_i(k+1) + (1 + T^2K_{\mathrm{P},i} - TK_{\mathrm{D},i})e_i(k) = 0 \tag{33}$$

The error dynamics is asymptotically stable whenever the zeros of all $i = 1, \ldots, 6$ polynomials

$$\lambda^2 + (TK_{\mathrm{D},i} - 2)\lambda + (1 + T^2 K_{\mathrm{P},i} - TK_{\mathrm{D},i}) = 0 \quad (34)$$

lie within the unit circle of the complex plane. Let those zeros be $\lambda_1$ and $\lambda_2$. Then $K_{\mathrm{D},i}$ and $K_{\mathrm{P},i}$ is given by

$$K_{\mathrm{D},i} = \frac{1}{T}(2 - \lambda_1 - \lambda_2) \quad (35)$$

$$K_{\mathrm{P},i} = \frac{1}{T^2}(\lambda_1\lambda_2 - \lambda_1 - \lambda_2 + 1) \quad (36)$$

Hence, for a deadbeat controller: $K_{\mathrm{D},i} = \frac{2}{T}$ and $K_{\mathrm{P},i} = \frac{1}{T^2}$.

## V. Disturbance Rejection

In general, disturbance $d(k)$ will not be constant or piecewise constant. In case of a measureable disturbance, using the extended nominal contol law

$$\gamma(k) = \bar{\gamma}(k) - J(\eta(k+1))M^{-1}d(k) \quad (37)$$

together with the compensator (30) then results in the nominal error dynamics (32). However, disturbances are not measurable in a realistic setup. Therefore, the controller shall further be extended for rejecting dynamic disturbances by means of an additional discrete observer to estimate the disturbance.

To this end, enhance (29) with the disturbance to obtain the disturbed discrete linear system

$$x(k+1) = A\,x(k) + B\,\gamma(k) + G(x(k))\,d(k) \quad (38)$$

where the state is defined as $x(k) := \begin{pmatrix} \eta(k) \\ \eta(k+1) \end{pmatrix} \in \mathbb{R}^{12}$ and

$$A = \begin{pmatrix} 0 & I \\ -I & 2I \end{pmatrix}, B = \begin{pmatrix} 0 \\ T^2 I \end{pmatrix}, G(x(k)) = \begin{pmatrix} 0 \\ T^2 J(x_2(k))M^{-1} \end{pmatrix}$$

with dimensions $A \in \mathbb{R}^{12\times 12}$ and both $B, G \in \mathbb{R}^{12\times 6}$.

In view of (38) define $\bar{d}(k) = G(x(k))\,d(k)$ and let $\hat{\bar{d}}(k)$ denote its asymptotic estimate. Then using the pseudo inverse and the disturbance estimate leads to the control law

$$\gamma(k) := \bar{\gamma}(k) - \frac{1}{T^2}(0 \quad I)\hat{\bar{d}}(k)\,. \quad (39)$$

For estimating the disturbance we devise a discrete version of a Generalized Extended State Observer (GESO) that we adopt from the design procedure for continuous time systems [9], [10], [11]. Along these lines, we treat the quantity $\bar{d}(k)$ in (38) as an extended system state in order to incorporate time derivatives of signal $\bar{d}(t)$ up to order $m$ in an extended system using a discrete Euler approximation [12]. Therefore, for the unknown disturbance $q_1(k) = \bar{d}(k)$ we have the dynamics

$$\begin{aligned} q_1(k+1) &= q_1(k) + T\,q_2(k) \\ q_2(k+1) &= q_2(k) + T\,q_3(k) \\ &\vdots = \vdots \\ q_{m-1}(k+1) &= q_{m-1}(k) + T\,q_m(k) \\ q_m(k+1) &= \bar{d}(k)^{(m)} \end{aligned}$$

These variables together with (38) define the extended state $\xi^{\mathrm{T}}(k) = [x_1^{\mathrm{T}}(k), x_2^{\mathrm{T}}(k), q_1(k), \ldots, q_m(k)] \in \mathbb{R}^{6(m+2)}$ of the extended system

$$\begin{aligned} \xi(k+1) &= A_{\mathrm{e}}\xi(k) + B_\gamma\gamma(k) + B_d\,\bar{d}(k)^{(m)} \\ y(k) &= C_{\mathrm{e}}\xi(k) \end{aligned} \quad (40)$$

with matrices

$$A_{\mathrm{e}} = \begin{pmatrix} 0 & I & 0 & 0 & 0 & \cdots & 0 \\ -I & 2I & T^2 I & 0 & 0 & \cdots & 0 \\ 0 & 0 & I & TI & 0 & \cdots & 0 \\ \vdots & \ddots & \ddots & \ddots & \ddots & \ddots & \vdots \\ 0 & \cdots & \cdots & \cdots & I & TI & 0 \\ 0 & \cdots & \cdots & \cdots & \cdots & I & TI \\ 0 & \cdots & \cdots & \cdots & & \cdots & 0 \end{pmatrix},$$

$$B_\gamma = \begin{pmatrix} 0 \\ T^2 I \\ 0 \\ \vdots \\ 0 \end{pmatrix}, B_d = \begin{pmatrix} 0 \\ 0 \\ \vdots \\ 0 \\ I \end{pmatrix}, C_{\mathrm{e}} = \begin{pmatrix} I & 0 & \cdots & 0 \end{pmatrix}$$

of appropriate size; $I$ and $0$ are $6 \times 6$ identity and zero matrices, respectively. Clearly, the pair $(C_{\mathrm{e}}, A_{\mathrm{e}})$ is observable and $y(k) = \eta(k)$ the measured output. As a consequence, the state $\xi(k)$ of the extended state space representation (40), thus also the unknown disturbance, may be estimated with an observer of the form

$$\hat{\xi}(k+1) = A_{\mathrm{e}}\,\hat{\xi}(k) + B_\gamma\,\gamma(k) + L\,(y(k) - C_{\mathrm{e}}\hat{\xi}(k)) \quad (41)$$

where the observer state $\hat{\xi}(k)$ denotes the estimate of state $\xi(k)$ and $L \in \mathbb{R}^{6(m+2)\times 6}$ is the observer gain. From (40) and (41) it is obvious that the estimation error dynamics reads

$$\tilde{\xi}(k+1) = (A_{\mathrm{e}} - L\,C_{\mathrm{e}})\,\tilde{\xi}(k) + B_d\,\bar{d}(k)^{(m)}$$

with estimation error $\tilde{\xi}(k) = \xi(k) - \hat{\xi}(k)$. Therefore, given that $\bar{d}(k)^{(m)}$ is bounded, $L$ serves for placing the eigenvalues of $A_{\mathrm{e}} - L\,C_{\mathrm{e}}$ in the unit circle of the complex plane, e.g. by using Ackermann's formula. Choosing the eigenvalues in the vicinity of the origin, the resulting observer forces the estimation error $\tilde{\xi}(k)$ to asymptotically converge to a small neighborhood of the origin of the error space. Finally, in control law (39) we may employ the disturbance estimate $\hat{\bar{d}}(k) = \big(\hat{\xi}_{13}(k), \ldots, \hat{\xi}_{18}(k)\big)$ for an asymptotic disturbance compensation.

## VI. Simulation results

In the simulations, we assume 11 way-points associated with their related longitudinal velocities as listed in Tab. I. Using the afore-presented algorithm these way points determine the path depicted in Fig. 3. Between the first and second way-point the vertical trajectory planning is considered, i.e. $\mathbf{z}_0 = 0$ and $\mathbf{z}_{\mathrm{f}} = 20$. Note that in the algorithm it is assumed that four way-points are known, that means, $\boldsymbol{\psi}_{\mathrm{f}} = \arctan\frac{y_{\mathrm{d}}'(0)}{x_{\mathrm{d}}'(0)} = 0.9409\,\mathrm{rad}$ and initial value $\boldsymbol{\psi}_0 = 0\,\mathrm{rad}$. When assuming a maximum velocity of $w_{\max} = 0.4\,\mathrm{m/s}$ we obtain $t_{\mathrm{f}} = \frac{15(\mathbf{z}_{\mathrm{f}} - \mathbf{z}_0)}{8w_{\max}} = 93.75\,\mathrm{sec}$. These generate the coefficients

for the the trajectories $z_{\mathrm{d}}(t)$ and $\psi_{\mathrm{d}}(t)$ using the relations (8), (9), (10) and (11), where $x_{\mathrm{d}}(t)$, $y_{\mathrm{d}}(t)$, $\phi_{\mathrm{d}}(t)$, and $\theta_{\mathrm{d}}(t)$ are all zero.

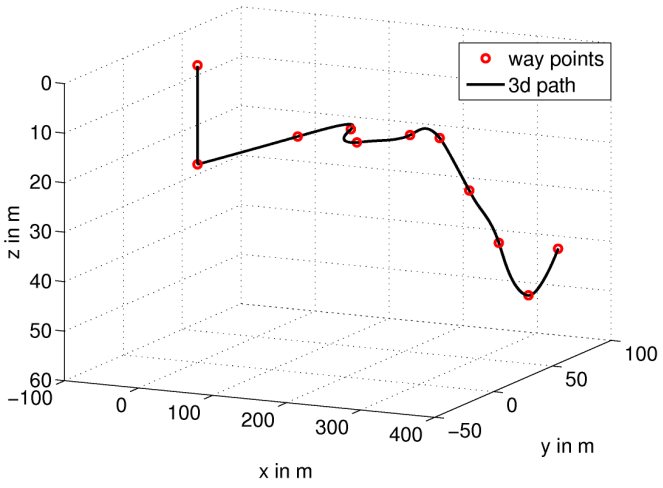


Fig. 3. Way points and desired path in underwater 3D space

The second phase of the motion planning starts at way-point two which is a stationary point. The 3D planning algorithm determines the intermediate paths, see Fig. 3, based on the desired way-point velocity data in such a way that $u_{\mathrm{d}}(t)$ is obtained as the low-pass filtered linear interpolation of $\theta$.

The controller is simulated referring to real-world data of an AUV that is available locally at the Institute of Automation and Systems Technology, Ilmenau University of Technology. For brevity, we omit the matrices $M$, $C$, and $D$ here. The mass of the AUV is $m = 132.535\,\mathrm{kg}$, length $L = 2.30$ m and radius $r = 0.15\,\mathrm{m}$, to give a rough idea about the dimensions. So as to investigate a realistic setting, we chose the sampling time as $T = 0.1$ sec. The discrete PD-controller is designed for eigenvalues $\lambda_1 = \lambda_2 = 0.95$, hence, with (35) and (36) we have $K_{\mathrm{D},i} = 1$ and $K_{\mathrm{P},i} = 0.25$ for $i = 1, \ldots, 6$.

In the simulation, we show two closed-loop scenarios: the nominal case (no disturbance) and the perturbed case.

*a) Nominal case:* Fig. 4 and Fig. 5 illustrate the tracking performance for position and orientation, respectively. The reference and resulting translational and angular velocities are shown in Fig. 6 and Fig. 7. The figures show that the reference trajectories generated by the path planner may be tracked with an acceptable control effort, see Fig. 8.

| # | 1 | 2 | 3 | 4 | 5 | 6 | 7 | 8 | 9 | 10 | 11 |
|---|---|---|---|---|---|---|---|---|---|---|---|
| x | 0 | 0 | 40 | 80 | 120 | 160 | 200 | 240 | 280 | 320 | 360 |
| y | 0 | 0 | 60 | 80 | 60 | 80 | 80 | 80 | 80 | 80 | 80 |
| z | 0 | 20 | 20 | 20 | 20 | 20 | 20 | 30 | 40 | 50 | 40 |
| u | 0 | 0 | 1 | 1 | 1 | 1 | 1 | 1 | 1 | 1 | 0 |

TABLE I
SPECIFIED WAY-POINTS FOR THE SIMULATION

*b) Perturbed case:* We assume a sinusoidal disturbance acting on the first and the sixth channel of the control input $\tau$, that is $d_1(t) = 10sin(2\pi 0.01)\,\mathrm{N}$ and $d_6(t) = 10sin(2\pi 0.01)\,\mathrm{Nm}$, which both are bounded as are its derivatives. The disturbance acts beginning from time $t = 300$ sec. The GESO is designed for $m = 4$. The eigenvalues of the estimation error dynamics, $A_{\mathrm{e}} - L\,C_{\mathrm{e}}$, are chosen all real with absolute value less than 0.1 such that the observation error dynamics decays faster than the controlled loop dynamics.

Comparing the resulting tracking performance with and without GESO when subject to these disturbances is shown in Fig. 9–12. It turns out that the tracking performance is remarkably improved when using the GESO while maintaining the control effort at approximately the same level, see Fig. 13 and Fig. 14. Note that for reducing the peaking-phenomenon after initializing, which may arise for high gain observers, we have used a "clutch" function for smoothing the transient peaking responses in the observer variables [13]. In our case, we have employed

$$s(t) = \begin{cases} 1 & \text{for} t > \varepsilon \\ \sin^q(\frac{\pi t}{2\varepsilon}) & \text{for} t \leq \varepsilon \end{cases}$$

for $q = 10$ and $\varepsilon = 6$.

## VII. CONCLUSION

We have presented a real-time path planning algorithm for the autonomous guidance of an AUV. Based on the recently conveyed way-ponts, the algorithm results in twice differentiable trajectories that are needed for the tracking controller. The algorithm is flexible enough such that when no further way-points are transmitted a stationary position may always be reached. The resulting trajectories may simply be tracked with a compensator-based PD-controller which is enhanced by a disturbance attenuation obtained from an extended state observer. Simulations with real-world data show that the tracking performance, when subject to disturbances, is acceptable. Future work will concentrate on the implementation of the algorithm on the locally available AUV, [14], for preparing an AUV-based sea water monitoring and management system.

## REFERENCES


[1] Y. Nakamura and S. Savant, "Nonlinear tracking control of autonomous underwater vehicles," in *Proc. of 1992 IEEE International Conference on Robotics and Automation*, 1992, pp. A4–A9.

[2] S. Arinaga, S. Nakajima, H. Okabe, A. Ono, and Y. Kanayama, "A motion planning method for an auv," in *Proc. of 1996 Symposium on Autonomous Underwater Vehicle Technology*, 1996, pp. 477–484.

[3] D. Fu-guang, J. Peng, B. Xin-qian, and W. Hong-jian, "Auv local path planning based on virtual potential field," in *Proc. of 2005 IEEE International Conference Mechatronics and Automation*, vol. 4, 2005, pp. 1711–1716.

[4] T. Fossen, *Marine Control Systems: Guidance, Navigation and Control of Ships, Rigs and Underwater Vehicles*. Marine Cybernetics, 2002.

[5] ——, "Nonlinear modelling and control of underwater vehicles," Ph.D. dissertation, Norwegian University of Science and Technology, 1991.

[6] ——, *Guidance and control of ocean vehicles*. John Wiley, 1994.

[7] H. Yuan and Z. Qu, "Optimal real-time collision-free motion planning for autonomous underwater vehicles in a 3d underwater space," *IET Control Theory & Applications*, vol. 3, no. 6, pp. 712–721, 2009.

[8] L. Biagiotti and C. Melchiorri, *Trajectory planning for automatic machines and robots*. Springer, 2008.

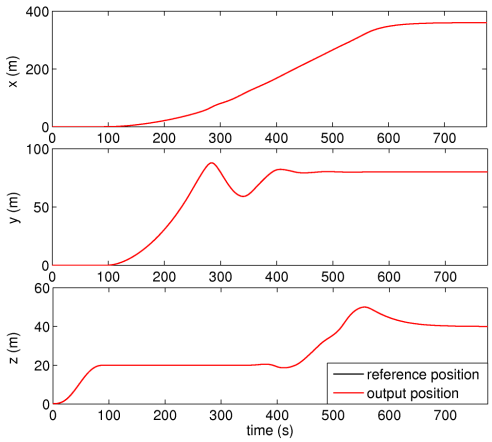


Fig. 4. Position

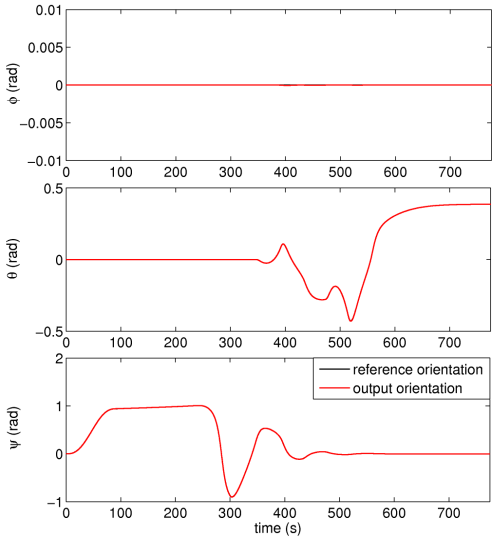


Fig. 5. Orientation


[9] J. Han, "From pid to active disturbance rejection control," *IEEE Transactions on Industrial Electronics*, vol. 56, no. 3, pp. 900–906, 2009.

[10] Z. Gao, "Active disturbance rejection control: A paradigm shift in feedback control system design," in *American Control Conference*, 2006, pp. 2399–2405.

[11] A. Radke and Z. Gao, "A survey of state and disturbance observers for practitioners," in *American Control Conference*, 2006, pp. 5183–5188.

[12] R. Miklosovic, A. Radke, and Z. Gao, "Discrete implementation and generalization of the extended state observer," in *American Control Conference*, 2006, pp. 2209–2214.

[13] H. Sira-Ramírez, "Robust linear output feedback control of a synchronous generator," in *American Control Conference*, 2011, pp. 3728–3733.

[14] M. Eichhorn, R. Taubert, C. Ament, M. Jacobi, and T. Pfützenreuther, "Modular auv system for sea water monitoring and management," in *Proc. of 2013 MTS/IEEE OCEANS, Bergen*, 2013.


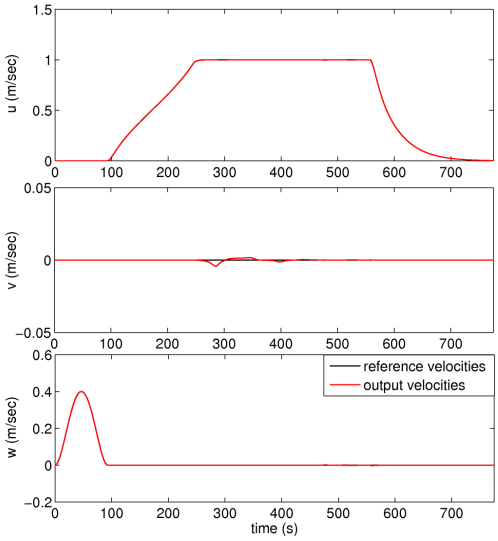


Fig. 6. Translational velocities

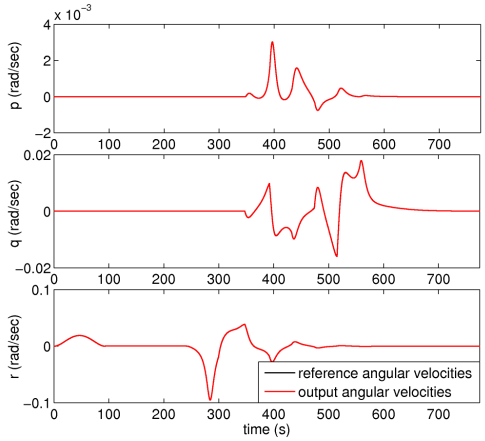


Fig. 7. Angular velocities

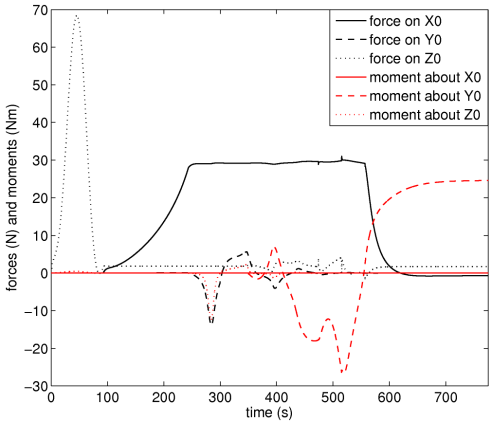


Fig. 8. Control input $\tau$, nominal case (PD-controller without observer)

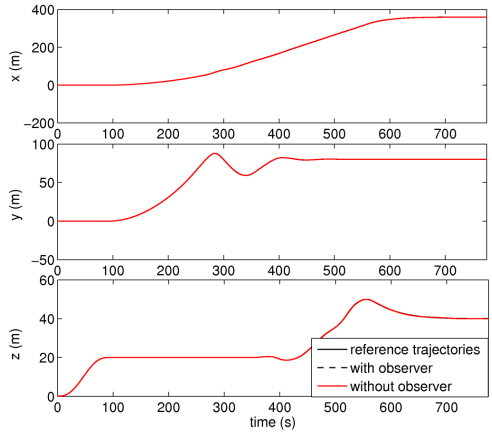


Fig. 9. Position under disturbance

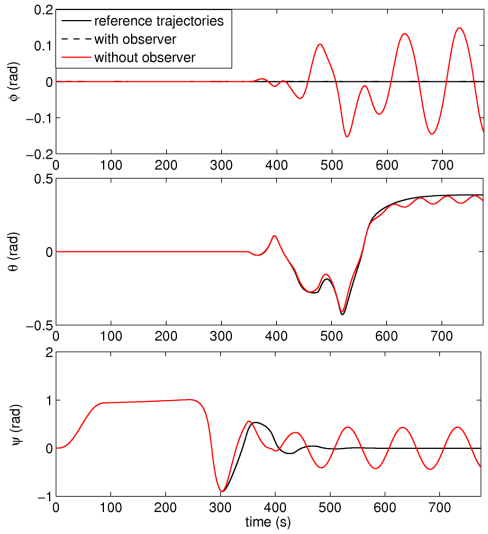


Fig. 10. Orientation under disturbance

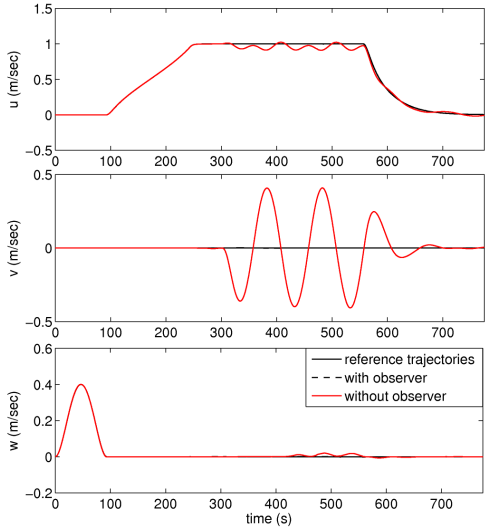


Fig. 11. Translational velocities under disturbance

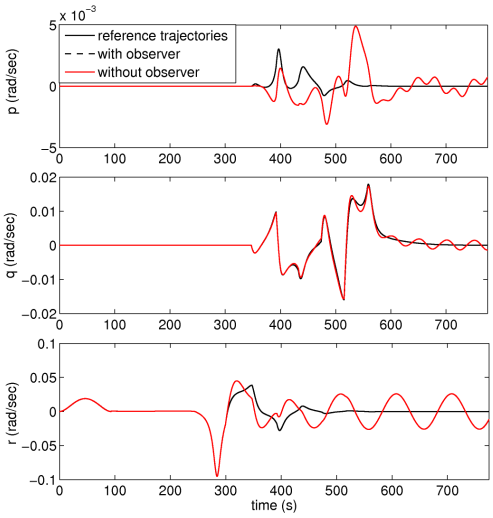


Fig. 12. Angular velocities under disturbance

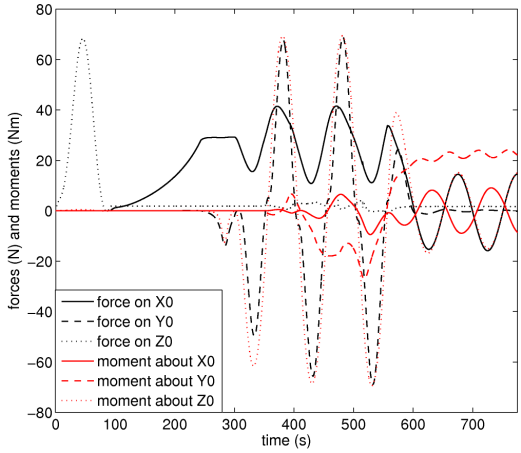


Fig. 13. Control input $\tau$, perturbed case (PD-controller without observer)

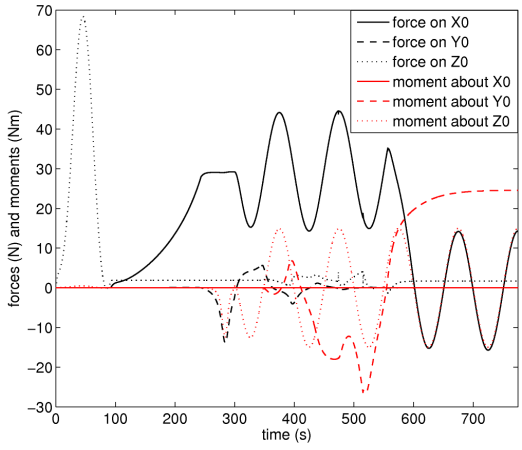


Fig. 14. Control input $\tau$, perturbed case (PD-controller with observer)